FUEL CONSUMPTION AND EMISSIONS ANALYSIS FOR A HYBRIDIZED VEHICLE

Jony Javorski Eckert[1], Fabio Mazzariol Santiciolli[1], Ludmila Corrêa de Alkmin e Silva[1], Eduardo dos Santos Costa[1], Elvis Bertoti[1], Fernanda Cristina Corrêa[2] and Franco Giuseppe Dedini[1]

[1]State University of Campinas - UNICAMP
[2]Federal Technological University of Paraná - UTFPR, Campus Ponta Grossa

E-mails: javorski@fem.unicamp.br, fabio@fem.unicamp.br, ludmila@fem.unicamp.br, eduardo.costa@fem.unicamp.br, bertoti@fem.unicamp.br, fernandacorrea@utfpr.edu.br, dedini@fem.unicamp.br

ABSTRACT

The improvement of the energetic efficiency in vehicular systems is a growing demand when developing new technologies for the automotive sector. Laws and regulatory standards that aim at the reduction of fuel consumption, such as the Brazilian INOVAR-AUTO, create constrains in order to improve the overall efficiency and reduce the emissions of new produced automobiles. Hybrid electric vehicles (HEVs) became an alternative to achieve these goals, by adding electricity as an auxiliary propulsion source. Several surveys have revealed the advantages of hybrid configurations, which demonstrated significant fuel savings resulting from shifting the engine operation point to regions of lower consumption. This study evaluates the impact of the conversion of a 1.0L vehicle into a plug-in electric vehicle (PHEV), by means of coupling electric motors supplied by lead-acid battery to the vehicle rear wheels (Parallel HEV Configuration). Thus, by means of simulations, this work aims to investigate the impact that the auxiliary electric system can produce in the fuel consumption and emissions of greenhouse gases when the vehicle is submitted to the standard Brazilian drive cycles NBR 6601 and NBR 7024.

INTRODUTION

The number of people who are adept to the means of private transportation has increased over the last decades. This number is strongly correlated with the number of automobiles in use on the roads around the world. If it is assumed that the automakers will follow on producing the majority of the cars equipped with conventional combustion engine, the fossil energy consumption and greenhouse gas (GHG) emissions will keep growing [1].

Plug-in hybrid vehicles (PHEVs) are gaining attention due to their ability to reduce gasoline/diesel consumption by using electricity from the grid as an alternative energy source [2]. If this energy is produced in a clean way and transmitted efficiently to the PHEVs' battery, it is possible to say that these vehicles are more environmental friendly than the conventional ones, considering all the resources spent per kilometer.

The studies performed were based on virtual models of a conventional car and a PHEV, both implemented through co-simulation using MATLAB/Simulink™ and ADAMS™, as well as emission data from ADVISOR™. These models are illustrated in Figure 1. The adopted conventional vehicle contains one Driver Interface that simulates the driver behavior based on the Brazilian drive cycles NBR 6601 and NBR 7024. This interface chooses which gear must be engaged and also inform the Power Management System (PMS) the expected throttle position. Then, the PMS controls the engine which drives the front wheel by means of a clutch, a gearbox and a differential.

The PHEV was built using the same platform of the conventional vehicle but adding a battery pack and two rear in-wheel motors. In this configuration, the PMS was expanded to include these new components in its management algorithms.

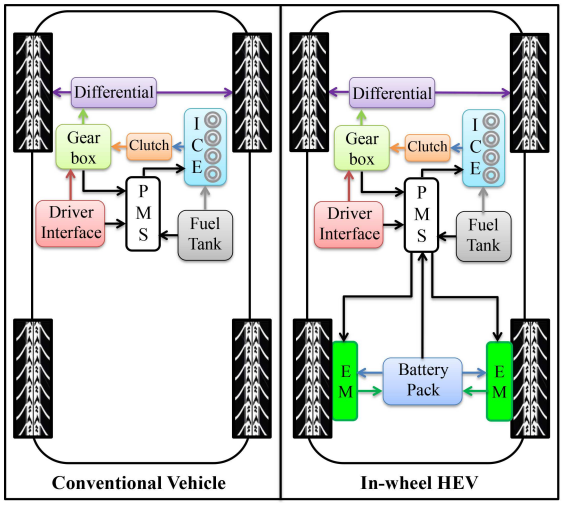

Figure 1 - Conventional and parallel hybrid vehicles adapted from [3]

The PHEV configuration chosen for analysis is known as “through-the-road” (TtR) HEV. This is a singular type of HEV because both sources of traction force are summed up “through the road” instead of combing them into one driveline (as it is done in the majority of the other PHEV configurations studied in the literature). It makes the complex torque coupling device unnecessary; making the implementation of this parallel HEVs simple and cheap. Furthermore, the 4-wheel drive capability provides more stability to the vehicle and exceptional acceleration. Finally, this feature represents the prospect of transforming any conventional ICE vehicle into a HEV. One disadvantage of this TtR HEV is the fact that the extra torque necessary to recharge the battery supplied from the ICE through the contact surface of the road is limited to the moments when vehicle is in motion [4].

In the present paper, based on these virtual models, the authors analyze the results of the sum of this extra electric drive system in a conventional vehicle, likewise the gear shifting strategy influences the vehicle behavior. The engine fuel consumption and emission are compared among four simulations models for each driving cycle. The first one corresponds to a conventional 1.0L Brazilian vehicle keeping the standard gear shifting strategy, provided by its manual. The second model also simulates the conventional vehicle, but with an improved gear shifting algorithm focused on fuel saving. The third and fourth models correspond to the PHEV simulations with the standard and the improved gear shifting strategies. Each model results in a distinctive engine regime that changes the fuel consumption and tailpipe emission that are strongly affected by the engine transient temperature phase.

1. VEHICLE LONGITUDINAL DYNAMICS

In the present studies, the simulations are based on the model proposed by [5] for the vehicle longitudinal dynamics. The Figure 2 shows the vehicle geometry parameters and the resistance forces that determine the vehicle power demand when it performs a given driving condition.

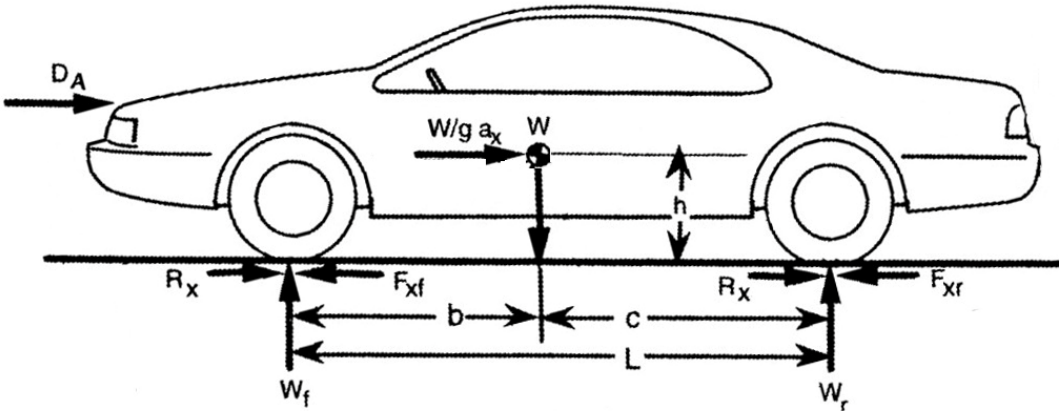

Figure 2 – Movement resistance forces and vehicle geometry, adapted from [5]

The requested torque at the vehicle propelling wheels T_{rw} [Nm] is determined in function of the vehicle mass M [kg] acceleration and the movement resistance forces, such as the tires rolling resistance (Rx) [N] and the aerodynamic drag (D_A) [N].

$$T_{rw} = \left(Ma_{req} + R_x + D_A\right)r \tag{1}$$

In this paper, the vehicle target speed is defined by standard driving cycles. Due to this, the required acceleration (a_{req}) [m/s^2] is given as the difference between the current vehicle speed (V) [m/s] and the driving cycle target speed (V_c) [m/s] divided by the simulation step size(dt) [s], as the Equation (2) shows.

$$a_{req} = \frac{V_c - V}{dt} \tag{2}$$

The aerodynamic drag (D_A) [N] originates from the air resistance imposed by the vehicle passage through it. This resistance force is the major factor of the power demand at high speeds, and it is estimated by the Equation (3) as a function of the vehicle frontal area A [m^2], air density ρ [kg/m^3], and an empirical constant known as drag coefficient (C_d), which varies according to the vehicle shape.

$$D_A = \frac{1}{2}\rho V^2 C_d A \tag{3}$$

On the other hand, at low speeds, the rolling resistance (R_x) [N] becomes the primary resistance load. This load corresponds to the tire energy loss due to the ground adhesion, and the contact area deformation, depending on the rubber damping properties. The rolling resistance is calculated by the Equation (4), as a function of the vehicle weight (W) [N].

$$R_x = 0.01\left(1 + \frac{2.24V}{100}\right)W \tag{4}$$

The climbing resistance is also responsible for a parcel in the vehicle power demand. The road angle changes the weight force component parallel to the ground, resulting in a force against the movement when the vehicle is going uphill, or a force that acts in favor of the movement when the vehicle is driving downhill [5]. However, in this work, the simulations follow the standard driving cycles NBR 6601 and NBR 7024, which does not provide information about the road grade during the cycles and, therefore, the climbing resistance is considered to be null during the driving cycles.

Once the required torque is defined, the vehicle available power sources will fulfill the demand by means of its propelling systems. In this paper, as mentioned before, two different vehicles are studied: the conventional one that is propelled by the ICE associated with a powertrain system with 5 available transition ratios and the PHEV model that presents similar ICE/powertrain system as the conventional vehicle, but with an extra electric propelling system coupled directly at the vehicle's rear wheels. For the conventional vehicle, the engine required torque (T_{re}) [Nm] is defined by the Equation (5) as a function of the gearbox (N_t) and differential (N_d) gear ratios, the powertrain overall efficiency (η_{td}) and the moment of inertias of each rotating component.

$$T_{re} = \frac{T_{rw} + \left((I_e + I_t)(N_t N_d)^2 + I_d {N_d}^2 + I_w\right)\frac{a_{req}}{r}}{N_t N_d \eta_{td}} \quad (5)$$

- r = Tire effective radius [m]
- I_e = Engine inertia [kgm^2]
- I_t = Gearbox inertia [kgm^2]
- I_d = Differential inertia [kgm^2]
- I_w = Wheels and Tires inertia [kgm^2]

However, during the gear shifting process, the engine is not allowed to transfer all the required torque T_{re} to the gearbox, due to the clutch decoupling from the rest of the powertrain [6]. This short period when the clutch disks are decoupled allows the gearbox to synchronize the next gear with the current power train speed. During the simulations, the gear shifting time of 1 second was adopted, as proposed by [7]. The gear shifting process is defined by [8] that set 0.3 s to complete engine decouple from the gearbox, followed by 0.2 s to change the gearbox transmission ratio, and 0.5 s to gradually recoupling the clutch discs, increasing the transmittable torque until it reaches the engine output torque. The clutch transmissible torque during the gear shifting process (T_{CL}) [Nm] is defined by the Equation (6), as given by [9].

$$T_{CL} = \frac{2}{3}\mu_{cl} F_n n \frac{{R_o}^3 - {R_i}^3}{{R_o}^2 - {R_i}^2} \quad (6)$$

- μ_{cl} = Clutch friction coefficient
- F_n = force applied between the discs [N]
- n = Clutch number of faces
- R_o = Clutch external disk radius [m]
- R_i = Clutch inner disk radius [m]

The vehicle acceleration performance is limited by two factors: restricted traction at start-up condition and low speed, as well as, available power to propel the vehicle [5] and [10]. The power limitation is given by the 100% throttle engine torque curve. The transmissible torque at

the tire/ground contact limits the vehicle acceleration to prevent the tires from slipping. To avoid performance losses caused by the tire/ground slipping, the simulation will use the maximum transmissible tire torque as a limit in the definition of the required torque T_{rw}. The vehicle traction limit is modeled as proposed in [11], as a function of the weight force acting on the vehicle axes, which may vary with the load transfers when the vehicle accelerates or brakes. Equations (7) and (8) show the maximum transmissible torque at the front $T_{f(max)}$ [Nm] and rear $T_{r(max)}$ [Nm] wheels, according to the tire-ground peak coefficient of friction (μ) and to the parameters related to the vehicle geometry.

$$T_{f(max)} = \mu\left(\frac{Wc}{2L} - \frac{Wha_x}{2Lg}\right) \tag{7}$$

$$T_{r(max)} = \mu\left(\frac{Wb}{2L} + \frac{Wha_x}{2Lg}\right) \tag{8}$$

- L = Wheelbase [m]
- h = Height of the vehicle's center of gravity [m]
- g = Gravity [m/s^2]
- b = Longitudinal distance between the vehicle's front axle and its gravity center [m]
- c = Longitudinal distance between the vehicle's rear axle and its gravity center [m]

The vehicle real acceleration (a_x) [m/s^2] used in the Equations (7) and (8) may be below the acceleration demand provided by the Equation (2), if the vehicle is limited by the tire traction limit or by the absence of torque, during the gear shifting process. For the conventional vehicle, the acceleration (a_x) is given by the Equation (9) as a function of the minimum torque value (T_{min}) [Nm], that is defined among the engine and tire limits. The first limit is the engine torque T_e [Nm] that could not fulfill the requested torque T_{re}, defined by the Equation (5), and become limited by the maximum torque curve of the engine; the available torque at the vehicle wheels T_w [Nm] is defined by the Equation (10) in function of the gearbox input torque T_g [Nm], that is also limited by the clutch transmissible torque during the shifting time T_{CL} (Equation (6)). The third limit is the tire transmissible torque $T_{f(max)}$ (for the frontal propelling system) that must be compared with the available wheel torque T_w.

$$a_x = \frac{\frac{T_{min}}{r} - R_x - D_A}{M} \tag{9}$$

$$T_w = T_{CL} N_t N_d \eta_{td} - \left((I_e + I_t)(N_t N_d)^2 + I_d {N_d}^2 + I_w\right)\frac{a_{req}}{r} \tag{10}$$

If the vehicle acceleration a_x resulting from Equation (10) is limited by the gearbox input torque or by the tire traction limit, presenting value below the required acceleration a_{req}, the simulation starts an interactive process among the Equations (5), (7) and (9) to establish the maximum possible acceleration value. After the convergence, the engine output torque T_e [Nm] is defined by the Equation (11), replacing the values of the required torque T_{rw} and acceleration a_{req} from the Equation (5), by the current values of torque T_{min} and acceleration a_x defined in the interactive procedure.

$$T_e = \frac{T_{min} + \left((I_e + I_t)(N_t N_d)^2 + I_d {N_d}^2 + I_w\right)\frac{a_x}{r}}{N_t N_d \eta_{td}} \tag{11}$$

For the PHEV configuration, the required torque T_{rw} defined by the Equation (1) is divided between the available propelling systems by a power management control (PMC). In this work, a simplified PMC algorithm is proposed, for which the electric propelling system is used as the primary drive system. In other words, if the required torque T_{rw} is bellow of the available EMs torque $T_{EM(max)}$ and the battery responsible to provide power to the EMs is not below the discharge limit, the vehicle will be propelled only by the electric system. In this case, the required torque T_{rw} is divided equally between the two EMs as shows the Equation (12).

$$T_{rEM} = \frac{T_{rw}}{2} \tag{12}$$

When the required torque T_{rw} overcomes the EMs capacity ($T_{rw} \geq T_{EM(max)}$) the combustion engine fulfills the remaining torque demand.

$$T_{rEM} = \frac{T_{EM(max)}}{2} \tag{13}$$

$$T_{re} = \frac{T_{rw} - T_{EM(max)} + \left((I_e + I_t)(N_t N_d)^2 + I_d {N_d}^2 + I_w\right)\frac{a_{req}}{r}}{N_t N_d \eta_{td}} \tag{14}$$

If the battery reaches the maximum allowed discharge limit, the PHEV will be propelled only by the ICE. The PHEV model also respects the tire traction, the clutch transmissible torque and the torque constraints of the propelling systems. For the PHEV, the calculation is similar to the one presented for the conventional vehicle, but the Equation (5) is replaced by the Equation (14), and the acceleration is then calculated by the Equation (15), instead of the Equation (9).

$$a_x = \frac{\frac{T_{min} + T_{Emin}}{r} - R_x - D_A}{M} \tag{15}$$

Where T_{Emin} [Nm] is the lowest torque value between the EMs required torque ($2T_{rEM}$) defined by the Equation (12) or (13) and the maximum transmissible torque at the vehicle rear wheels calculated by the Equation (8). In this case, the interactive algorithm that defines the vehicle acceleration a_x uses the Equations (7), (8), (12), (13), (14), (15) and (16). If the EMs required torque T_{rEM} overcomes the traction limit of the rear tires ($2T_{rEM} > T_{r(max)}$), the value of $T_{r(max)}$ will replace T_{rw} in the Equation (12) or replace $T_{EM(max)}$ in the Equation (13) and the remaining torque will be fulfilled by the ICE drive system.

2. SIMULATION PARAMETERS

The simulations were performed by an integration between the multibody dynamic analysis program Adams™ and the Simulink/Matlab ™ which provides an interface to control the multibody vehicle model by means of the Adams™ plugin Adams/Controls™ as proposed in [3]. The set of equations described previously were implemented in Simulink™ to estimate the vehicle power demand, the gear shifting strategy, and the power split between the ICE and electric systems for the PHEV simulations.

The simulated vehicle is based on a 1.0L Brazilian vehicle and the standard gear shifting strategy is the one proposed by [12] that defines the standard vehicle speeds when the gear shifting should occur. The vehicle parameters used in the simulations are shown in Table 1.

Some modifications on these parameters related to the PHEV model are properly described in the analysis of the electric drive system.

Table 1 - Vehicle parameters [8].

Components	**Units**	**Speed**					**Vehicle Geometry**	
		1st	**2nd**	**3rd**	**4th**	**5th**		
Engine inertia	Kgm^2	0.1367					Vehicle frontal area	1.8 m^2
Gearbox inertia ($\times 10^{-4}$)	Kgm^2	17	22	29	39	54	Drag coefficient	0.33
Gearbox ratios	-	4.27	2.35	1.48	1.05	0.8	Wheelbase	2.44 m
Differential inertia	Kgm^2	9.22E-04					Gravity center height	0.53 m
Differential ratio	-	4.87					Rear axle to gravity center	1.46 m
Wheels + tires inertia	Kgm^2	2					Front axle to gravity center	0.98 m
Conv. vehicle mass	kg	980					Tire peak friction coefficient	0.9
Tires	-	175/70R13					Tire radius [m]	0.2876
Clutch external radius	mm	95					Clutch friction coefficient	0.27
Clutch internal radius	mm	67					Clutch faces (n)	2

3. PHEV ELETRIC DRIVE SYSTEM

The PHEV analyzed is based on a conventional 1.0L engine vehicle with two 5 kW electric motors coupled to the vehicle's rear wheels (parallel HEV), as proposed by [13]. The electric motors were modeled as from [14] with voltage of 48 V between their terminals but as in-wheel motors, i.e., without any reduction coupling the motor to the wheel. Therefore, the simulations consider the EMs torque characteristics equivalent to the resultant torque and speeds in the vehicle wheels as from the assembly proposed by [13]. The EMs efficiency map is estimated based on the EM described in [15]. The Figure 3 shows the original and equivalent in-wheel EMs torque curves and the efficiency map for the in-wheel EM used during the simulations.

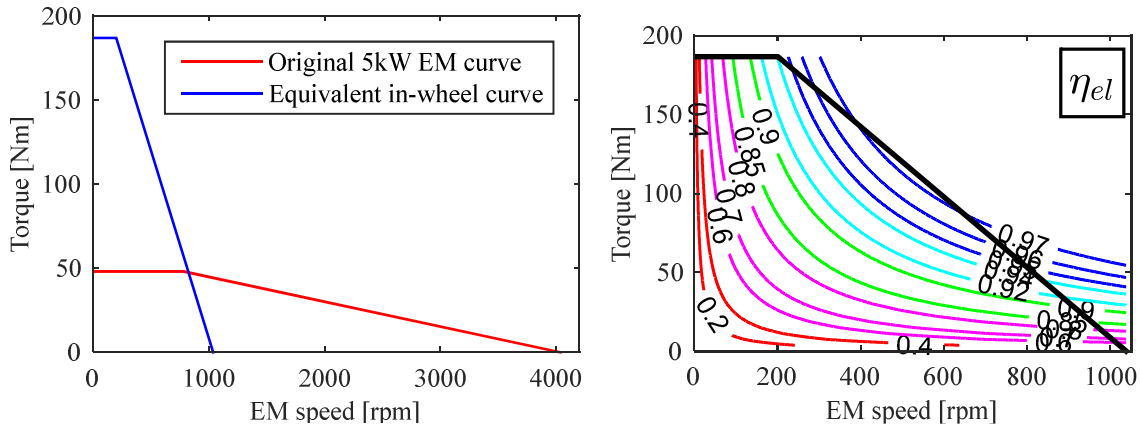

Figure 3 – Electric motors torque curve and efficiency map.

The electric system current I [A] is calculated by Equation (17), as a function of the torque at the electric motors T_{rEM} defined by the Equation (12) or (13), the instantaneous EM speed ω_{EM} [rad/s], the battery output voltage V [V], the EM (η_{el}) and inverter (η_{inv}) efficiencies provided by Figure 3 and Table 2.

$$I = \frac{2\,T_{rEM}\omega_{EM}}{V\eta_{el}\eta_{inv}} \quad (17)$$

Table 2 - Inverter efficiency η_{inv} adapted from [16]

T_{EM} [Nm]	ω_{EM} [rad/s]				
	105	**314**	**524**	**733**	**942**
0	0.65	0.84	0.90	0.84	0.83
0.11 T_{max}	0.74	0.89	0.94	0.91	0.91
0.33 T_{max}	0.82	0.93	0.96	0.96	0.96
0.56 T_{max}	0.83	0.94	0.97	0.97	0.97
T_{max}	0.83	0.94	0.97	0.97	0.97

The current I defined by the Equation (17) discharges the four PHEV batteries, which are similar to the 12 V lead-acid battery proposed in [13] and they are connected in series to provide the 48 V required by the EMs. This battery pack provides 100 Ah of charge and increases the mass of the vehicle in 120 kg. The battery simulation is based on the Simulink™ database lead-acid battery, using the equations described in [17] and keeping the same parameters used in the previously described battery pack.

Since the modeled hybrid vehicle is a PHEV, the battery starts the simulation fully charged by the electrical grid. The battery may also be recharged during the driving cycles by regenerative braking, i.e., when the electric motors act as generators, converting the kinetic energy of the vehicle into electricity [18], allowing the vehicle to recover part of the energy that would be wasted during decelerations and storing it in the batteries [19]. During the simulations, the EMs regeneration capacity will be considered as 5% of the EM maximum torque curve. The remaining braking torque demanded is supplied by the friction brake system that guarantees the vehicle deceleration performance requirements [20].

To avoid premature damage in the batteries that can be caused by theirs complete discharge [21], the battery state of charge SoC have to be limited. Thus, the vehicle must discharge the battery until it reaches a minimum SoC of 30%–45% depending on battery type and on the powertrain configuration [2], [22]. In this paper the battery SoC is limited to 40% as in [3].

To define the PHEV total mass for the simulations it is considered the conventional vehicle mass (980kg) plus the 120 kg from the battery pack and the addition of 30 kg relative to the EMs and inverters. Then, the PHEV total mass becomes 1130 kg.

4. ENGINE SIMULATION

The ICE (Internal Combustion Engine) is modeled using the maps and simulation model provided by ADVISOR™ (Advanced Vehicle Simulator) [23]. Several papers as [2], [22] and [24] use the ADVISOR™ models as reference to compare fuel consumption and emission simulations results. The engine specific fuel consumption map and the CO, NO_x and HC emission maps of the ADVISOR™ conventional default vehicle are shown in Figure 4. These are emissions maps after treatment of catalyst parameters for a hypothetical gasoline-powered engine in transient regime obtained from tests performed according to FTP standards and, therefore, they are only appropriate to simulation models that consider the engine transient-operation [23].

The Adams/Simulink™ co-simulation stores the engine operation points (torque and speed) synchronized with the time vector. These results are used as an input to the engine simulation of ADVISOR™, which defines the fuel consumption and emissions according to the set of parameters defined by the its algorithm. Among these parameters, the most important is the engine temperature, that strongly influences the emissions degree. The engine simulation starts at ambient temperature set to 20 °C and it is heated by the combustion model until it reaches the operation temperature of 95 ± 5 °C, which is controlled by the engine coolant system.

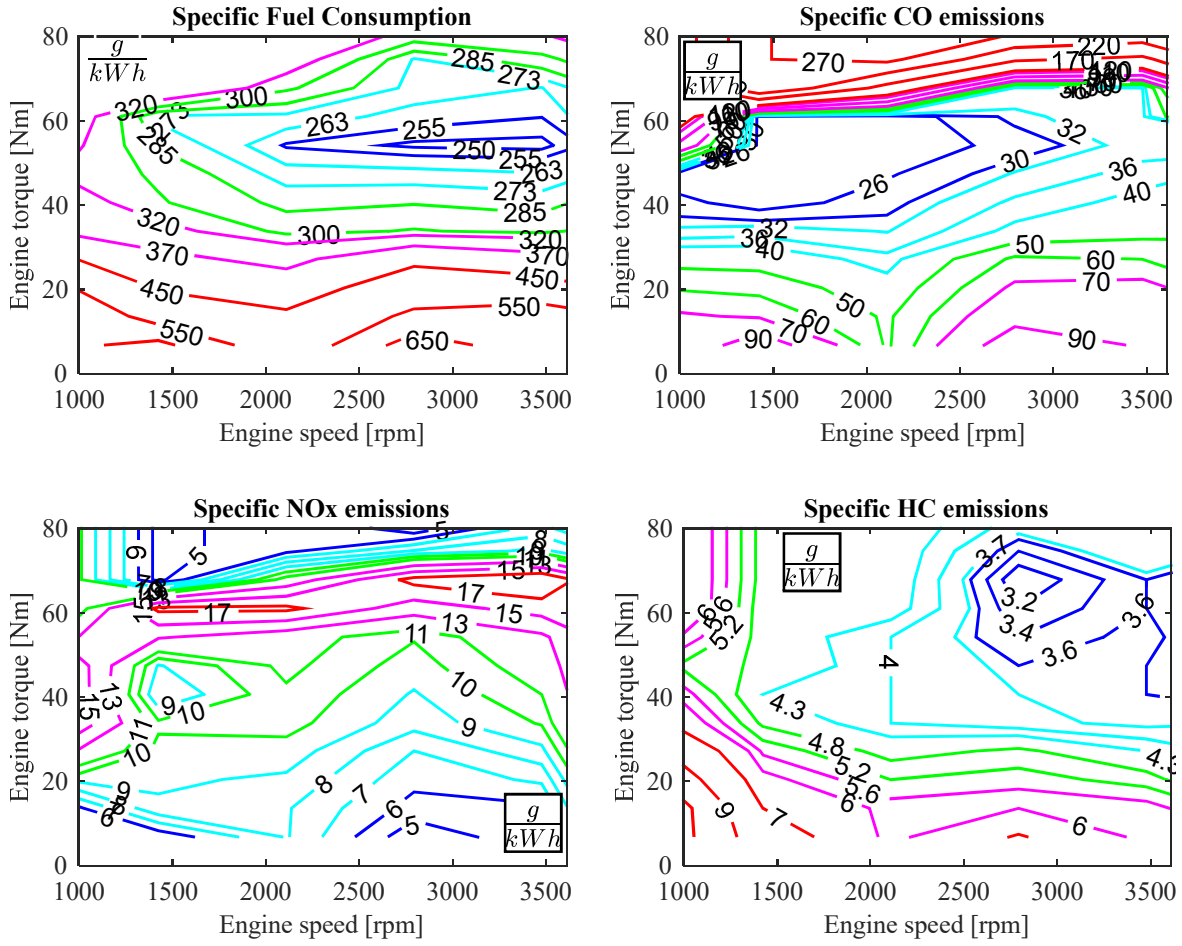

Figure 4 – Engine fuel consumption and emission maps [23].

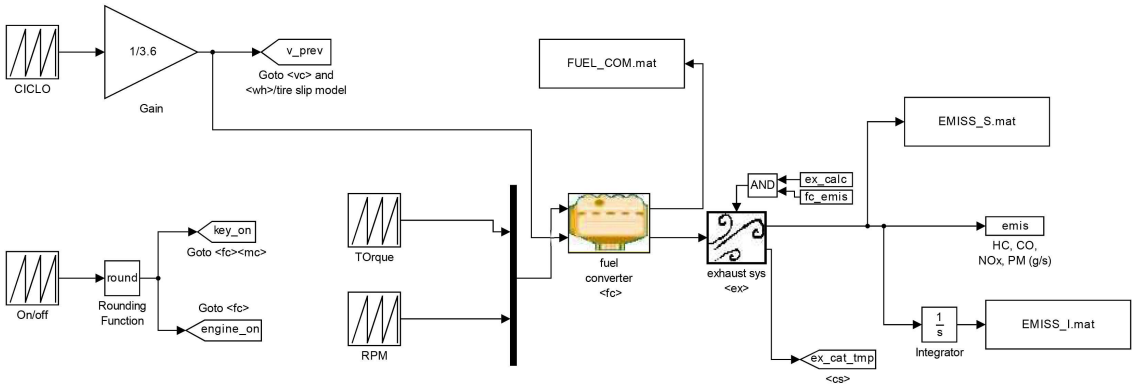

Figure 5 – ADVISOR™ engine model. Adapted from [23]

The engine thermal model divides the engine assembly into four temperatures: cylinders, engine block, exterior engine accessories, and the vehicle hood [23]. The heat, generated by combustion, is conducted to the engine block and removed through forced liquid cooling, conduction, natural convection, and radiation [23].

The final tailpipe emissions are the result of engine output emissions multiplied by the total effective catalyst efficiency. The catalyst temperature is calculated based on the correlation coefficients that estimate the heat transferred by convection from the gas to the components, and from the components to the environment [23].

5. DRIVING CYCLES AND EMISSION STANDARDS

The vehicle required acceleration determined by the Equation (2) is defined by comparing the current vehicle speed with standard velocities profiles defined by the driving cycles. The simulations are performed considering the NBR 6601 Brazilian urban driving cycle [25] and the NBR 7024 Brazilian highway driving cycle [26], which are shown in Figure 6.

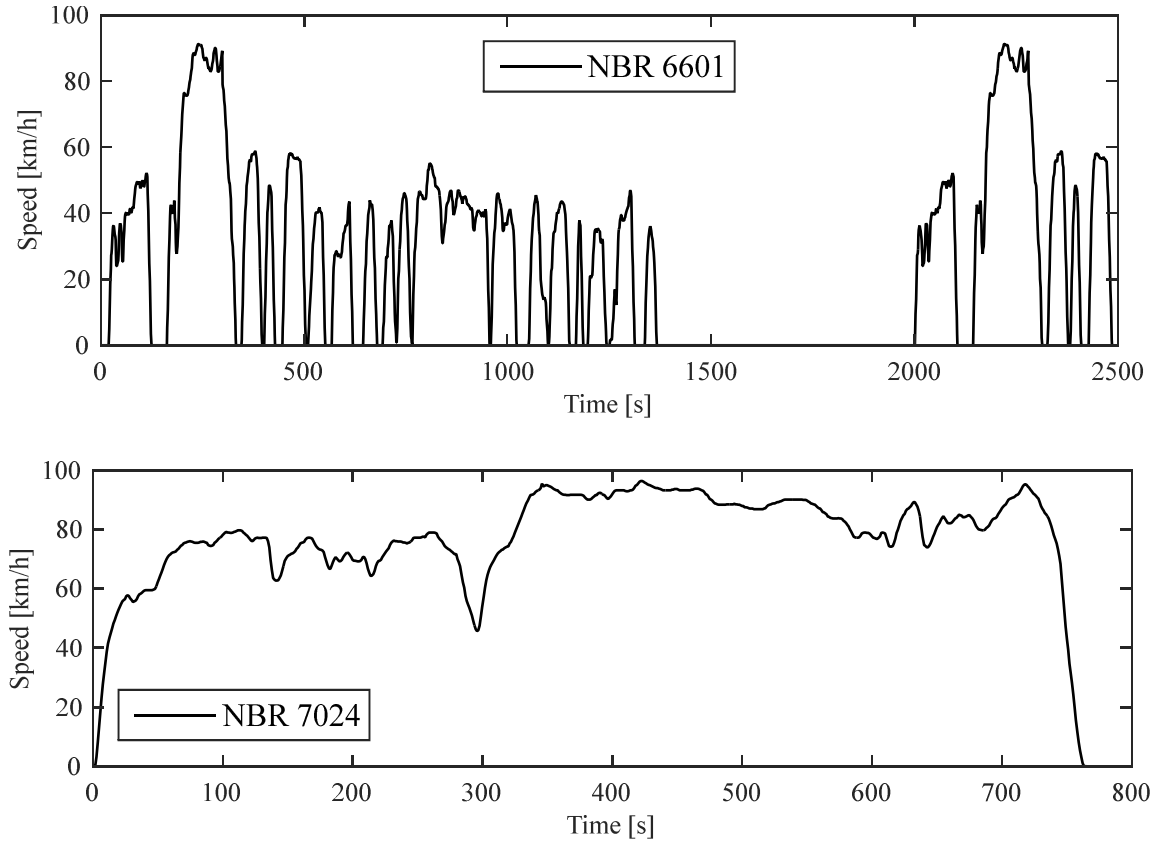

Figure 6 –Standard driving cycles NBR 6601 [25] and NBR 7024 [26].

The emission standard NBR 6601 is defined by cold and hot start experiments. The cold start is divided into two phases: the first one stars at the beginning of the cycle and goes until 505 s; the second corresponds to the stabilized engine regime going from 505 s to 1371 s. The hot start experiment is performed after the end of the cold start one and also after a period in which the engine is turned off. The hot start stabilized phase is similar to the cold start stabilized phase and therefore it does not need to be completely executed: because the major part of the pollutants are emitted during the transient regime, especially at cold start part. The emission

limits for passenger vehicles are shown in Table 3, and they are according to the rules defined in 2003 and 2014.

Table 3 – Brazilian emission limits for light vehicles [27]

POLLUTANTS	Maximum emission limits			
	2003	2007	2009	2014
Carbon monoxide CO	2.0 [g/km]	2.0 [g/km]	2.0 [g/km]	1.3 [g/km]
Nitrogen oxides NOx	0.6 [g/km]	0.16 [g/km]	0.12 [g/km]	0.08 [g/km]
Hydrocarbons HC	----	0.25 [g/km]	0.05 [g/km]	0.05 [g/km]

6. GEAR SHIFTING STRATEGY

The gear shifting strategy influences the vehicle acceleration performance and also fuel consumption because it changes the powertrain inertia and the engine speed [8]. During the simulations, a standard gear shifting strategy proposed by [12] defines the vehicle speeds for which the changes of each gear must happen. This strategy presents satisfactory results when performed in the NBR 6601 driving cycle as shown in [28], but it can be further improved by anticipating the upshift and putting the engine to operate in a more efficient region of its consumption map.

Experimental results from [13] demonstrated that the extra electric power added to the vehicle by the EMs reduces the engine required torque, allowing the PHEV to perform an earlier upshift as compared with the conventional vehicle. The simulations for the conventional vehicle and the PHEV are performed using the standard gear shifting strategy and also the gear shifting algorithm developed by [29], that analyses the ICE required torque and performs an upshift, if it is possible, to fulfill the power demand using the next available gear.

To avoid performance losses generated by the interruption of the engine torque supply caused by the clutch decoupling/recoupling process, a dwell time between two subsequent gear shifts is implemented in the algorithm as suggested by [30], in order to prevent several consecutive gear shifts.

7. RESULTS

As commented previously, two simulations were performed for each vehicle, the first adopting the standard gear shifting strategy and the second with the modified gear shifting algorithm. The fuel consumption and emissions for the NBR 6601 driving cycle are shown in Table 4.

Table 4 - Simulation results for the NBR 6601 driving cycle.

Results	Units	Simulated Vehicles			
		Conventional	Conventional+ Gear shifting	PHEV	PHEV+ Gear shifting
Traveled Distance	km	17.43	17.28	17.79	17.75
Fuel Consumption	l	1.4451	1.3292	0.8435	0.6634
Consumption Average	km/l	12.06	12.99	21.09	26.76
CO	g/km	2.9191	3.1276	1.0307	0.9365
NOx	g/km	0.1815	0.1995	0.0803	0.0992
HC	g/km	0.2848	0.2910	0.1880	0.1956
SoC	%	-----	-----	55.57	55.71

Analyzing the results obtained for the conventional vehicle, it is possible to observe that the vehicle travelled was 17.43 km, which represents 360 m of distance less than the cycle total length of 17.79 km. This difference is caused by the speed decrease that occurs during the gearshifts. About the engine fuel consumption for the conventional vehicle, it will be set as the reference value for the comparative amongst all simulated cases. With respect to the emissions, the conventional vehicle presented results close to the limits established by [27] for the year of 2007, but the carbon monoxide CO values are above the limits already proposed in 2003. It happens basically because the engine fuel consumption and emission maps simulated in this papers are based on a 2002 engine data, as documented in [23].

The PHEV simulations presented improvements in vehicle performance, by reaching a final travel distance close to the total length of the cycle due to the extra electric in-wheel motors that continued to propel the vehicle during the gearshifts, reducing or even eliminating the speed decrease caused by the clutch decoupling. This happens because the proposed PHEV electric drive system acts independently of the engine/powertrain system. Considering now the application of the modified gear shifting strategy improved the fuel consumption in both models. However, the final travelled distance decreased as compared with the respective vehicle when using the standard gear shifting strategy, because more frequent gearshifts decrease the vehicle performance.

To better analyze the differences between the simulated vehicles, their engine operation points are shown in the Figure 7. It is possible to observe that the PHEV simulation resulted in expressive decrease in the engine required torque, presenting only few points close to the engine maximum output torque (100% throttle). The second observed behavior is in respect of the gear shifting strategy: the modified gear shifting algorithm that anticipates the upshift process moves the operation points for the engine lower speeds and also higher torque as compared to the respective vehicle using the standard gear shifting tactic.

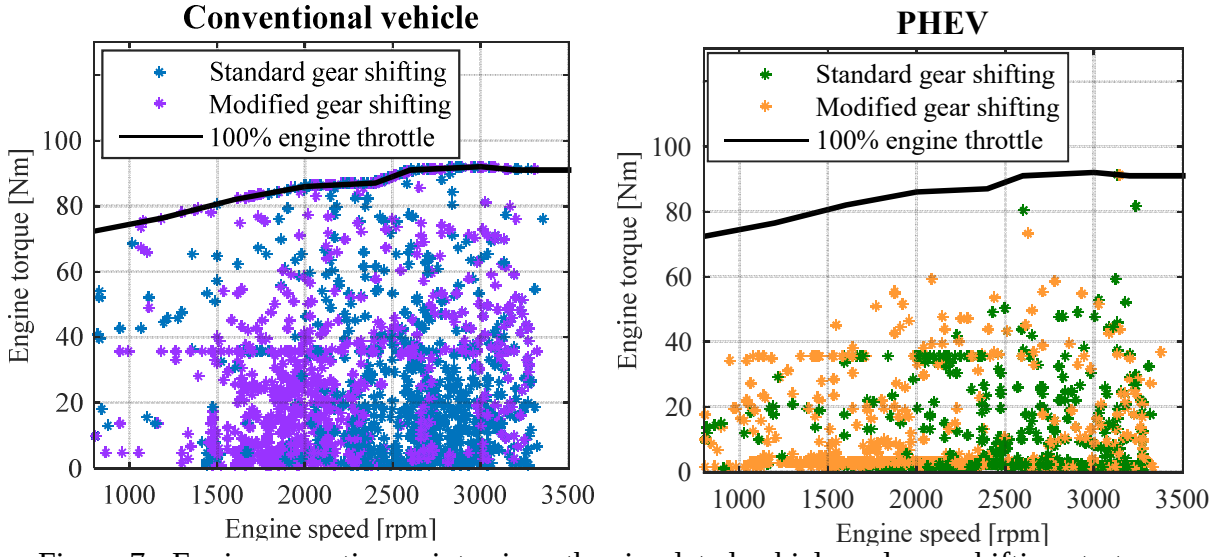

Figure 7 - Engine operation points given the simulated vehicle and gear shifting strategy

The results shown in Figure 7 represent the engine behavior during the NBR 6601 driving cycle, however, it is difficult to analyze the simulation outcomes over the engine fuel consumption and emissions maps, because there are several superposed points that could generate incorrect interpretation of the engine behavior. To facilitate the analyses of the engine operation point the tactic used previously in [29] is adopted. The method consists in locating the smallest

rectangular region that concentrates 75% of the engine operation points. This rectangular region is defined by an interactive algorithm, which starts with the whole set of engine torque and speed values. They must be compensated to represent similar weights in the minimum rectangle area definition. The vertices of the rectangle values are changed randomly, and the resulting area is compared to the previous results, and if the rectangle does not contain at least 75% of the engine point this result is discarded. The process is repeated several times until the convergence of the minimum rectangle that keeps 75% of the operation points.

The fuel consumption and emission maps are analyzed in two different modes in this paper. The first one is the original format that shows the amount of consumed fuel (or generated emission gas) by operation time and output power that characterize the specific maps. The second way to analyze the engine maps is given by decoupling the engine power from the map output, once the power is represented in the point definition (torque [Nm] × engine speed [rad/s]). Each point of the specific map is multiplied by its respective power in kW, generating maps that show the fuel/emission by amount of time [g/h] according to the operation point. For the fuel consumption the fuel mass is converted into volume [l] by dividing the mass [g] by the fuel density [g/l]. The Figure 8 shows the engine specific and volumetric fuel consumption maps, and also the rectangles defined by the four simulated cases that represent the location of the majority of operation points.

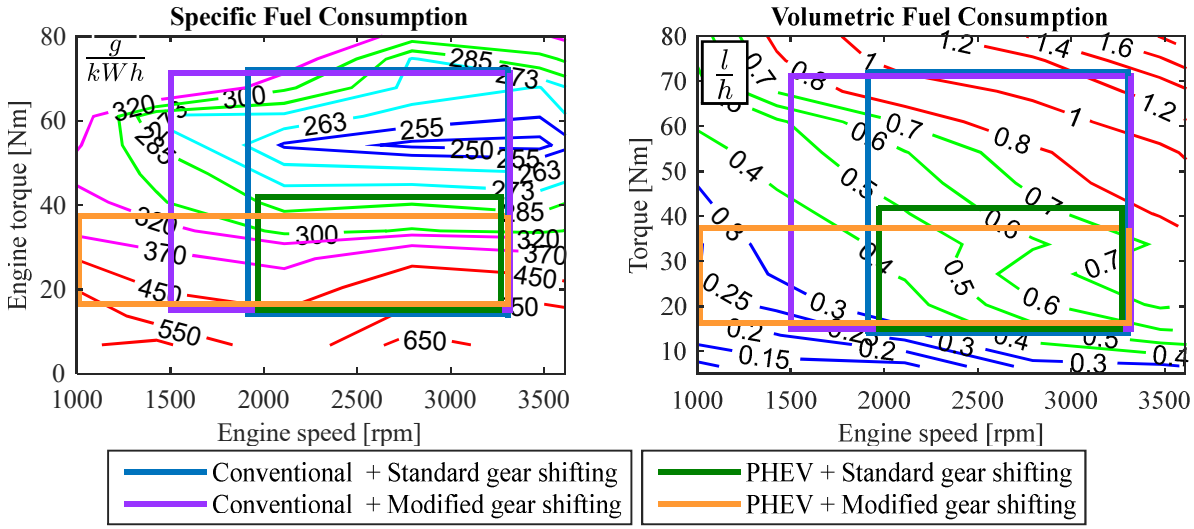

Figure 8 - Engine fuel consumption maps

As observed in Table 4, by changing the conventional vehicle gear shifting strategy the engine fuel consumption decreased 115.9 ml (8.02%). Observing the specific fuel consumption map from Figure 8 is possible to conclude that the modified gear shifting strategy moves the operation point to a lower engine speed region that represents an efficiency decrease in relation to the output power by amount of fuel consumed. However, if the same effect is analyzed in the volumetric fuel consumption map, the modified gear shifting strategy moves the engine operation points to a lower volumetric fuel consumption region that represents the fuel saving using this gear shifting strategy.

Similar analyses could be made for the PHEV as compared with the conventional vehicle. The result from Table 4 shows a 41.63% fuel saving as compared with the conventional and the PHEV using the standard gearshift strategy, and 49.91% fuel saving comparing both models using the modified gear shifting algorithm. Now, observing only the PHEV simulation output

without the modified gear shifting effect (green rectangle) the engine operation points were moved to the low torque regime, because one parcel of the required torque is now provided by the EMs propelling system. Similar to the analysis of the gear shifting effect, the operation points for the PHEV engine represent an efficiency decrease in the specific fuel consumption map, but also moved to a lower fuel consumption region in the volumetric map, which explains the fuel saving results depicted in Table 4. Finally, the PHEV that uses the modified gear shifting strategy presents the minimum fuel consumption because it combines the effect of the electric drivetrain, which reduces the engine torque, and simultaneously anticipates upshift, which moves the operation point for a lower volumetric fuel consumption region.

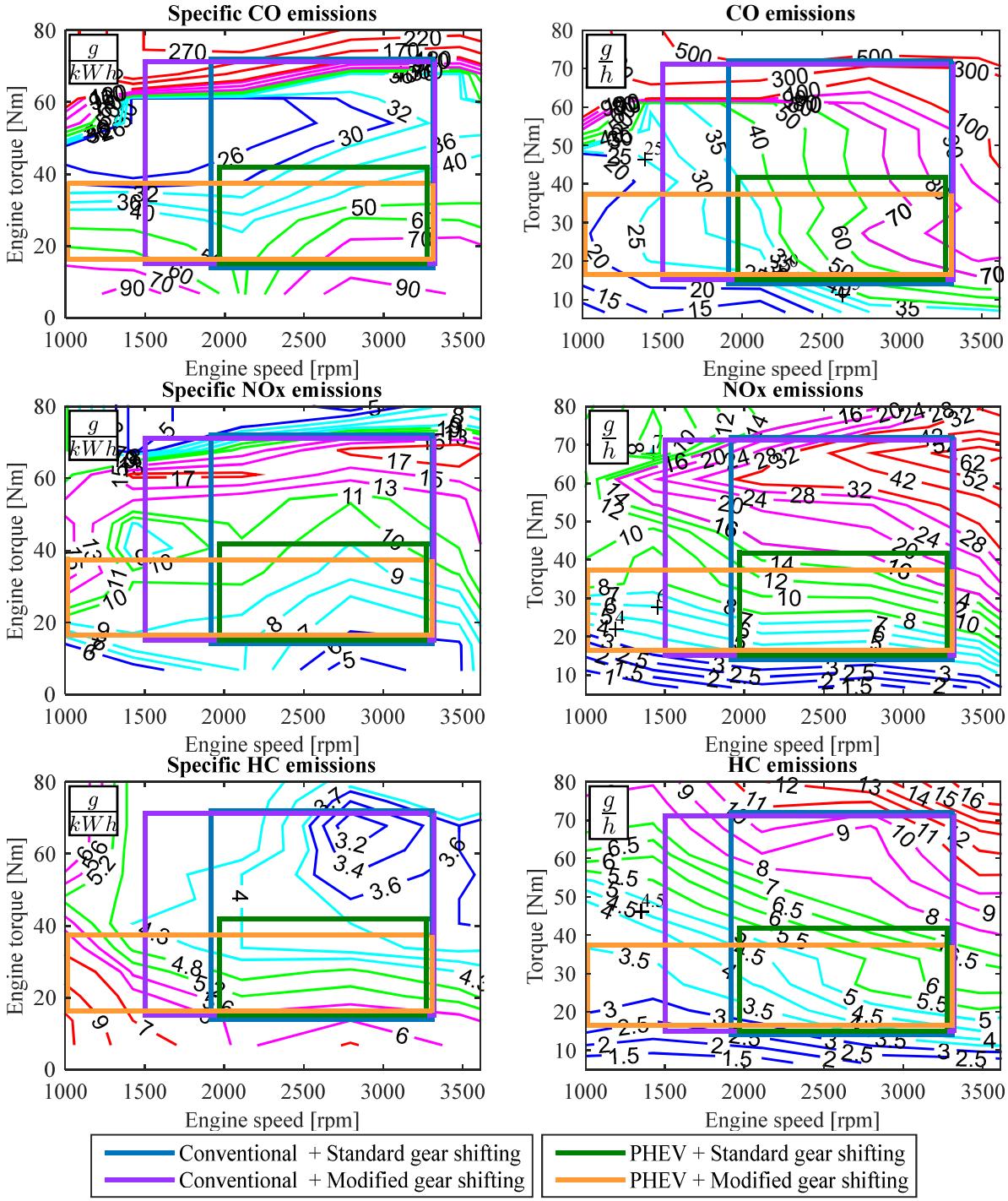

Figure 9 - Engine emissions maps

It is important to emphasize that the PHEV fuel consumption savings must be compensated, because the electric energy used to charge the battery pack represents a cost that must be converted in equivalent fuel consumption and added in the final PHEV engine consumption to determine the real gain offered by the PHEV as compared with the conventional vehicle [2]. However, this kind of analysis is not the focus of this paper and, due to this, the comparatives are based on the results from Table 4 without any correction coefficient.

Analyzing the engine emissions for the conventional vehicle, it is observable that the alternative gear shifting strategy moves the engine operation points to a region that outputs more pollutants, as shown in the g/h maps in Figure 9. In some cases, by visual analyses, the shift in the engine operation point seems not to change the emission region values, especially in the g/h maps. However, Table 4 shows that the emissions increases for all the analyzed tailpipe gases (+7.14% CO +9.92% NOx and +2.18% HC) from the conventional vehicle with modified gear shifts, as compared to the standard strategy.

This effect is explained by the reduction of the engine speed with the anticipation of the upshift, which reduces the combustions in the engine cylinder, and consequently the generated heat. In the PHEV simulation, the decrease in the requested torque also reduces the generated engine heat, and therefore, increases the time needed so that the engine reaches its ideal working temperature. The engine temperature during the NBR 6601 cycle is shown in Figure 10. It is possible to observe that the combination between the electric motor and the modified gear shifting strategy delays the warming-up of the engine.

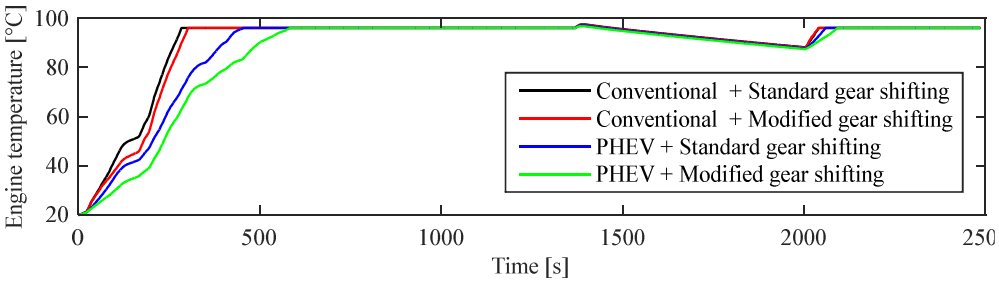

Figure 10 – Engine warm-up for the four simulations

As described previously, the engine emissions maps were obtained from transient regime data, and corrected as function of the engine temperature. This effect can be noticed from Table 5 which shows the emission in the cold starts phase (0 to 505 s) presenting much higher values, as compared with the remaining cycle excerpts. Due to this effect, the modified gear shifting strategy increases the emission in the conventional vehicle, because it increases the engine warming-up interval, increasing the pollutant emissions while the engine does not reach the temperature of stabilization, as shown in Figure 10.

On the other hand, the PHEV needs even more time to reach the engine stabilized regime, but presents lower emissions values compared to the conventional vehicle, and differently of the conventional vehicle, the PHEV presents the best results using the modified gear shifting strategy analyzing the final result from Table 4. It happens because the emission reduction by the change of engine operation point (Figure 9) overcomes the effect of the low engine temperature that increases the emissions, until the engine reaches the appropriate temperature. At the same time, the gain of the modified gear shifting strategy applied to the PEHV must be evaluated according to analyzed tailpipe gas and cycle phase, because in some cases the use of the standard gear shifting strategy presents better results as could be observed in the Table 5.

The employed gear shifting strategies are show in Figure 11. One may see that the modified shift tactic anticipate the upshift, increasing the usage of the 4th gear during the cycle. The results for the hot start phase are similar to the cold start simulation in the cycle beginning. In the PHEV simulation the vehicle does not need to use the 1st gear because the addition of the extra electric power enables the PEH to fulfill the required startup torque by engaging directly the 2nd gear.

Table 5 - Emission according to the cycle phase

Cycle phases	**Emissions**	**Simulated Vehicles**			
		Conventional	Conventional+ Gear shifting	PHEV	PHEV+ Gear shifting
Cold start 0 to 505 s	CO [g]	40.2409	42.3874	14.9194	13.7061
	NOx [g]	1.8041	2.0859	0.9541	1.2938
	HC [g]	3.5247	3.6546	2.5303	2.6944
Stabilized engine 505 to 1371 s	CO [g]	4.7587	5.1665	1.6432	1.3156
	NOx [g]	0.7069	0.7284	0.2388	0.2288
	HC [g]	0.7758	0.7317	0.4339	0.4008
Hot start 2000 to 2486 s	CO [g]	5.8708	6.4780	1.9563	1.7867
	NOx [g]	0.6518	0.6326	0.2501	0.2583
	HC [g]	0.6632	0.6418	0.4141	0.4154

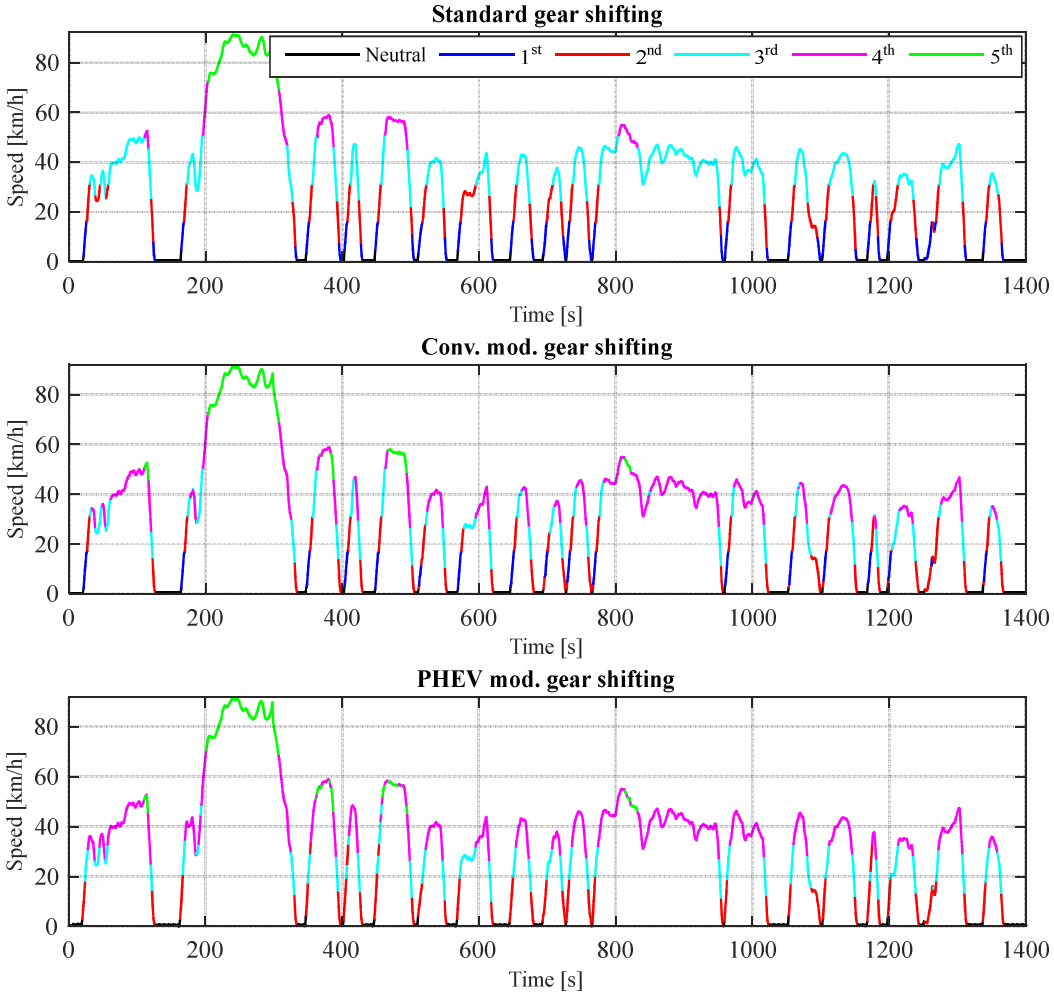

Figure 11 - Gear shifting strategies

Finally, the resulting emission from all the simulated vehicles are compared to the standard emissions limits shown in Table 3. As described before, the conventional vehicle presents higher emission levels than the limits imposed in 2003, because the simulate engine data is based on a model of a 2002 engine. Considering the PHEV model, the emissions presented an expressive reduction. The CO emissions are 20.71% below the limit when using the standard gear shifting strategy and 27.96% below when the modified strategy is employed. Analyzing the NOx emissions, the PHEV outputted an outcome very closer to the 2014 NOx maximum limit when using the standard gear shifting strategy; but when the modified strategy is used the result is 24% above the same limit. The worst outputs presented by the simulated vehicles are related to the HC emission that oversteps the 2007 maximum tolerances; the best obtained result (PEH+ standard gearshift) is still 2.7 times higher than the 2014 restrictions. On the other hand, the HC emission decreases 33.99% as compared to the conventional vehicle results.

The same simulations were performed for the NBR 7024 driving cycle that characterizes the vehicle highway driving behavior. The results obtained for this cycle can be seen in Table 6. It is noticeable that the PHEV model presented an expressive reduction in the fuel consumption (43.07%) and also a reduction in the engine emissions. Since the NBR 7024 is no more adopted as a standard to evaluate vehicle emissions, the results for this cycle are only to perform comparisons amongst the simulated vehicles and cannot to be compared with the restrictions established in Table 3.

Table 6 - Simulation results for the NBR 7024 driving cycle.

Results	**Units**	**Simulated Vehicles**			
		Conventional	Conventional+ Gear shifting	PHEV	PHEV+ Gear shifting
Traveled Distance	km	16.4616	16.4554	16.5225	16.5226
Fuel Consumption	l	0.9138	0.9094	0.5188	0.5093
Consumption average	km/l	18.0154	18.0941	31.8470	32.4408
CO	g/km	3.2275	3.2604	1.0142	0.9678
NOx	g/km	0.1782	0.1928	0.0550	0.0588
HC	g/km	0.2659	0.2709	0.1561	0.1583
SoC	%	-----	-----	63.67	63.69

Comparing the data from Table 4 with the outcomes from Table 6, it is possible to observe that the same tendencies related to the engine fuel consumption and pollutant emissions are still present for the cycle given by the NBR 7024. The only exception relies on the NOx emissions, which increased by the selection of the modified gear shifting strategy, in opposition to what happened for the NBR 6061.

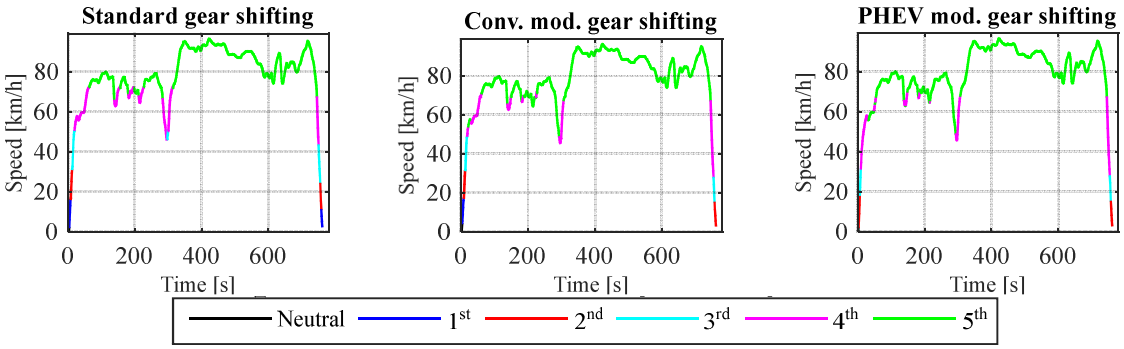

Figure 12 - Gear shifting strategies in the NBR 7024 driving cycle

Despite of that, the modified gear shifting strategy shows less influence in the NBR 7024 cycle when compared to the results for the NBR 6601 cycle. This might be due to the fact that highway driving cycles has a long path of high speed with only a few gear shifts between the top and the 4th gear transmission ratios, as could be observed in Figure 12. The effect of the reduced number of gearshifts during the cycle can also be observed by the closer overall travelled distance resulted from all simulations.

CONCLUSION

In this paper, it was studied the influence of the electric hybrid vehicle technology in the engine fuel consumption and emissions. The effects of an improved gear-shifting algorithm were also evaluated. The engine operation regime (torque and speed) is acquired from the simulation of the vehicle longitudinal dynamics, and it provides the input data for the engine simulation based on the ADVISOR^{TM} engine model and its maps, which made possible the calculation of the fuel consumption and emissions for a 1.0L engine.

The simulations were based on the Brazilian standard driving cycles NBR 6601 and NBR 7024 and the results are compared with the regulated emission standards. The PHEV simulation shows an expressive improvement of the vehicle fuel consumption and also reductions in the tailpipe emission. The use of an improved gear shifting algorithm that reduces the fuel consumption by anticipating the upshift, only presented improvements for some pollutant emissions, depending on the simulated vehicle and cycle excerpt.

The PHEV fuel consumption improvement must be compensated by estimating an equivalent fuel consumption that compensates the cost of the electric energy used to charge the PHEV battery. This equivalent fuel consumption must be added to the final engine consumption to define the real gain of the PHEV as compared with the conventional vehicle.

Finally, it is concluded that the employment of electric motors as an auxiliary propelling system in the vehicle allowed the engine to spare fuel, by reducing its torque demand and, therefore, allowing an anticipated upshift which moved the operation point to a lower consumption region. By operating the engine at lower torque regime, the PHEV tailpipe emission are also reduced even with the engine slower warming-up period. Due to this fact, the next step will be to optimize the PHEV system and its gear shifting strategy to find out the most adequate power split between the combustion and electric power sources, which can minimize not only fuel consumption, but also pollutant emissions and simultaneously the battery discharges.

ACKNOWLEDGEMENTS

This work was conducted during scholarships supported by the Brazilian Federal Agency for Support and Evaluation of Graduate Education (CAPES), National Council for Scientific and Technological Development (CNPq) and the State University of Campinas (UNICAMP).

REFERENCES

[1] ZHOU, Xuesong, TANVIR, Shams, LEI, Hao, TAYLOR, Jeffrey, LIU, Bin, ROUPHAIL, Nagui M, et al. Integrating a simplified emission estimation model and mesoscopic dynamic traffic simulator to efficiently evaluate emission impacts of traffic management strategies. **Transportation Research Part D: Transport and Environment**. 2015;37:123-36.

[2] SILVA, Carla, ROSS, Marc, FARIAS, Tiago. Evaluation of energy consumption, emissions and cost of plug-in hybrid vehicles. **Energy Conversion and Management**. 2009;50(7):1635-43.

[3] ECKERT, Jony J, SANTICIOLLI, Fabio M, SILVA, Ludmila CA, COSTA, Eduardo S, CORRÊA, Fernanda C, DEDINI, Franco G. Co-simulation to evaluate acceleration performance and fuel consumption of hybrid vehicles. **Journal of the Brazilian Society of Mechanical Sciences and Engineering**. 2016:1-14.

[4] SABRI, MFM, DANAPALASINGAM, KA, RAHMAT, MF. A review on hybrid electric vehicles architecture and energy management strategies. **Renewable and Sustainable Energy Reviews**. 2016;53:1433-42.

[5] GILLESPIE, Thomas D. **Fundamentals of Vehicle Dynamics**. 1st ed. Engineers SoA, editor. Warrendale, Pa., USA1992 february 1992. 495 p.

[6] NAUS, GJL, BEENAKKERS, MA, HUISMAN, RGM, VAN DE MOLENGRAFT, MJG, STEINBUCH, M. Robust control of a clutch system to prevent judder-induced driveline oscillations. **Vehicle System Dynamics**. 2010;48(11):1379-94.

[7] YIN, Xiaofeng, XUE, Dianlun, CAI, Yun, editors. Application of time-optimal strategy and fuzzy logic to the engine speed control during the gear-shifting process of AMT. **Fuzzy Systems and Knowledge Discovery, 2007 FSKD 2007 Fourth International Conference on**; 2007: IEEE.

[8] ECKERT, Jony Javorski, CORRÊA, Fernanda Cristina, SANTICIOLLI, Fabio Mazzariol, COSTA, Eduardo dos Santos, DIONÍSIO, Heron José, DEDINI, Franco Giuseppe. Vehicle gear shifting strategy optimization with respect to performance and fuel consumption. **Mechanics Based Design of Structures and Machines**. 2016;44(1-2):123-36.

[9] KULKARNI, Manish, SHIM, Taehyun, ZHANG, Yi. Shift dynamics and control of dual-clutch transmissions. **Mechanism and Machine Theory**. 2007;42(2):168-82.

[10] SPANOS, PD, CASTILLO, DH, KOUGIOUMTZOGLOU, IA, TAPIA, RA. A nonlinear model for top fuel dragster dynamic performance assessment. **Vehicle System Dynamics**. 2012;50(2):281-97.

[11] JAZAR, Reza N. Vehicle Dynamics. **Theory and Applications Riverdale, NY: Springer Science+ Business Media**. 2008.

[12] GM. Owner Manual Chevrolet Celta 2013. General Motors Brazil Ltda; 2013.

[13] COSTA, Eduardo Dos Santos, ECKERT, Jony Javorski , SANTICIOLLI, Fabio Mazzariol, DIONÍSIO, Heron José, CORRÊA, Fernanda Cristina, DEDINI, Franco Giuseppe. **Computational and Experimental Analysis of Fuel Consumption of a Hybridized Vehicle** SAE Technical Paper; 2014.

[14] GOLDEN MOTOR. Brushless DC Motor Instructions. In: Co.Ltd. GMT, editor. http://www.goldenmotor.com/eCar/HPM48-5000Curve.pdf: Golden Motor; 2016.

[15] ECKERT, Jony Javorski, CORRÊA, Fernanda Cristina, SANTICIOLLI, Fabio Mazzariol, DOS SANTOS COSTA, Eduardo, DIONÍSIO, Heron José, DEDINI, Franco Giuseppe. An influence study of parallel hybrid vehicle propulsion system configurations. **Blucher Engineering Proceedings**. 2015;2(1):62-81.

[16] ROTERING, Niklas, ILIC, Marija. Optimal charge control of plug-in hybrid electric vehicles in deregulated electricity markets. **Power Systems, IEEE Transactions on**. 2011;26(3):1021-9.
[17] Implement generic battery model [Internet]. 2016. Available from: http://www.mathworks.com/help/physmod/sps/powersys/ref/battery.html;jsessionid=d013bc50994ddeb54d1b7ae5bbc8.
[18] JUNZHI, Zhang, YUTONG, Li, CHEN, Lv, YE, Yuan. New regenerative braking control strategy for rear-driven electrified minivans. **Energy Conversion and Management**. 2014;82:135-45.
[19] LV, Chen, ZHANG, Junzhi, LI, Yutong, YUAN, Ye. Mechanism analysis and evaluation methodology of regenerative braking contribution to energy efficiency improvement of electrified vehicles. **Energy Conversion and Management**. 2015;92:469-82.
[20] ZHANG, Junzhi, LV, Chen, GOU, Jinfang, KONG, Decong. Cooperative control of regenerative braking and hydraulic braking of an electrified passenger car. **Proceedings of the Institution of Mechanical Engineers, Part D: Journal of Automobile Engineering**. 2012:0954407012441884.
[21] FUHS, Allen. **Hybrid Vehicles: and the Future of Personal Transportation**: CRC Press; 2008.
[22] SILVA, CM, FARIAS, TL, FREY, H Christopher, ROUPHAIL, Nagui M. Evaluation of numerical models for simulation of real-world hot-stabilized fuel consumption and emissions of gasoline light-duty vehicles. **Transportation Research Part D: Transport and Environment**. 2006;11(5):377-85.
[23] AARON, Brooker, HARALDSSON, Kristina , HENDRICKS, Terry , JOHNSON, Valerie , KELLY, Kenneth , KRAMER, Bill , et al. ADVISOR: a systems analysis tool for advanced vehicle modeling. http://adv-vehicle-sim.sourceforge.net/2013.
[24] MONTAZERI-GH, Morteza, POURSAMAD, Amir, GHALICHI, Babak. Application of genetic algorithm for optimization of control strategy in parallel hybrid electric vehicles. **Journal of the Franklin Institute**. 2006;343(4):420-35.
[25] ABNT, NBR 6601. Light road motor vehicles - Determination of hydrocarbons, carbon monoxide, nitrogen oxides, carbon dioxides and particulate matter in the exhaust gas. 2012.
[26] ABNT, NBR 7024. Light road vehicles - Fuel consumption measurement - Test method. 2010.
[27] INOVAR-AUTO. Programa de Incentivo à Inovação Tecnológica e Adensamento da Cadeia Produtiva de Veículos Automotores. http://www.planalto.gov.br/CCIVIL_03/_Ato2011-2014/2012/Decreto/D7819.htm2012.
[28] ECKERT, Jony Javorski, SANTICIOLLI, Fabio Mazzariol, COSTA, Eduardo S, CORRÊA, Fernanda Cristina, DIONÍSIO, Heron José, DEDINI, Franco Giuseppe. Vehicle gear shifting co-simulation to optimize performance and fuel consumption in the brazilian standard urban driving cycle. **Blucher Engineering Proceedings**. 2014;1(2):615-31.
[29] CORREA, Fernanda C, ECKERT, Jony J, SILVA, Ludmila CA, COSTA, Eduardo S, SANTICIOLLI, Fabio M, DEDINI, Franco Giuseppe, editors. Gear Shifting Strategy to Improve the Parallel Hybrid Vehicle Fuel Consumption. **Vehicle Power and Propulsion Conference (VPPC), 2015 IEEE**; 2015: IEEE.
[30] CASAVOLA, Alessandro, PRODI, Giovanni, ROCCA, Giuseppe, editors. Efficient gear shifting strategies for green driving policies. **American Control Conference (ACC), 2010**; 2010: IEEE.